Time-resolved microphotoluminescence of epitaxial laterally overgrown GaN

J. Holst,[a] A. Kaschner, and A. Hoffmann
Institut für Festkörperphysik, Technische Universität Berlin, 10623 Berlin, Germany

P. Fischer, F. Bertram, T. Riemann, and J. Christen
Institut für Experimentelle Physik, Otto-von-Guericke-Universität, 39016 Magdeburg, Germany

K. Hiramatsu
Department of Electrical and Electronic Engineering, Mie University, Mie 514-8507, Japan

T. Shibata and N. Sawaki
Department of Electronics, Nagoya University, Nagoya 464-01, Japan

(Received 2 June 1999; accepted for publication 23 September 1999)

Epitaxial laterally overgrown GaN (ELOG) structures are microscopically characterized using spatially resolved microphotoluminescence (micro-PL) and time-dependent spectroscopy. To understand the influence of the different lateral growth mechanisms on the peak position and the temporal behavior of the transition lines, we correlated the different micro-PL emission spectra with results of spatially resolved time-dependent spectroscopy experiments. © *1999 American Institute of Physics.* [S0003-6951(99)04846-9]

The group-III nitrides and their related ternary alloys have been becoming the most attractive material for light-emitting diodes and laser diodes in the UV and blue spectral range.[1] Recently, laser diodes with an estimated lifetime of more than 10 000 h were reported.[2] To achieve such lifetimes, the introduction of the epitaxial lateral overgrowth (ELO) technique was claimed to be effective. This method has already been applied successfully in reducing dislocation density in the GaN layers on sapphire substrates.[3] A correlation of the optical properties with local strain and free-carrier concentration of ELOG structures oriented along the $\langle 1\underline{1}00\rangle$ and $\langle 11\underline{2}0\rangle$ directions is described in Refs. 4 and 5. In this letter, we focus on the correlation of optical properties of ELOG having SiO_2 masks in the $\langle 1\underline{1}00\rangle$ (sample A) and $\langle 11\underline{2}0\rangle$ (sample B) direction, and the resulting carrier dynamics.

The ELOG samples investigated here are schematically drawn in Figs. 1(a) and 2(a). A detailed description of the sample structures is given in Refs. 4 and 5. The microphotoluminescence (micro-PL) setup is described in Ref. 6. A spatial resolution better than 600 nm is achieved under optimum conditions. The micro-PL measurements were carried out in backscattering geometry and the signal was collected into a 0.5 m spectrometer and a charge-coupled device camera. For time-dependent photoluminescence the signal was analyzed in a 0.35 m subtractive double spectrometer and detected by a microchannel plate photomultiplier. A single-photon-counting setup was used. Employing convolution techniques, the overall time resolution is 15 ps.

In Figs. 1 and 2 local micro-PL spectra and scanning electron microscopy (SEM) images of the samples are depicted. We make a distinction between the overgrown regions above the SiO_2 masks and the area of coherent growth among the stripes. We recorded a series of spectra and the corresponding transients along lines from the sample's surface to the substrate interface in both regions.

Seen on the $\langle 1100\rangle$ plane, the coherently grown region in sample A forms a uniform monochromatic rectangle up to the surface where a sharp excitonic luminescence at 358.6 nm dominates all spectra. In the overgrown region of this sample the local spectra change appreciably: one moves closer to the SiO_2 masks and the free exciton at 358.0 nm and the donor-bound exciton (D_0X) at 358.6 nm are clearly resolved in the spectrum at 20 μm from the mask. 3 μm above the SiO_2 mask a luminescence on the high-energy side of the excitonic lines occurs, which is due to band-to-band recombination. The free-carrier concentration in this area is above the Mott density, which is confirmed by micro-Raman.[5] This can be explained by the fact that the coalescence area lies exactly above the SiO_2 masks. From this high carrier concentration a transition from excitonic to band-to-band recombinations is observed. In the overgrown region of sample B the micro-PL is dominated by a D_0X luminescence at 358 nm and a broad blueshifted emission at 354 nm due to band-to-band transitions is observed. The emissions in the coherently grown region are of excitonic origin, but slightly broadened with increasing distance from the substrate.

To correlate the time-resolved measurements and the spatial distribution of luminescence centers, local micro-PL measurements are collected at the same positions as the transient. Luminescence transients taken in the energy range of the donor-bound exciton lines of the samples are shown in the Figs. 1(c) and 1(d) (sample A) and 2(c) and 2(d) (sample B) for the overgrown region and coherently grown region, respectively. The partial overlap of the recombination lines of the free and the donor-bound excitons due to the spectral window of 5 nm during the time-resolved measurements requires a careful analysis of the transients. It was carried out using the convolution of the system response to the laser

[a]Electronic mail: holsten@physik.tu-berlin.de

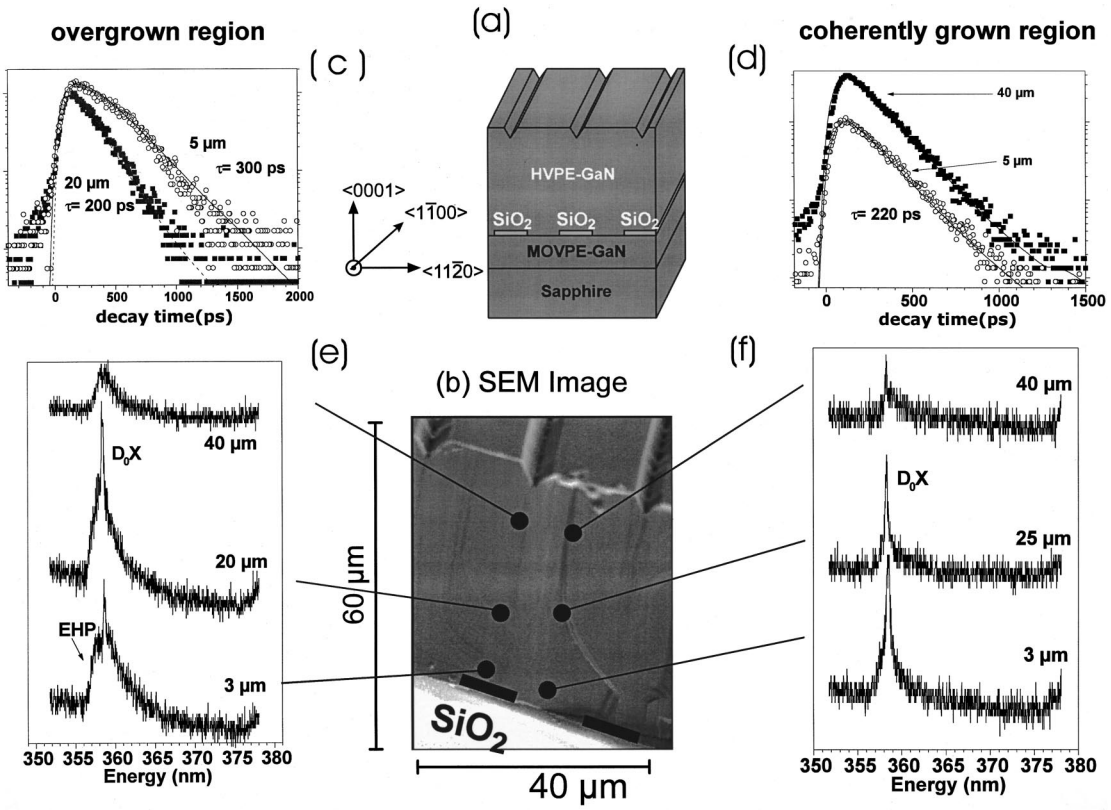

FIG. 1. Schematic structure of ELOG sample B with the SiO_2 pattern along the $\langle 1\underline{1}00\rangle$ direction (a) together with a SEM image (b) and transients taken at 358 ± 5 nm for different distances from the masks of the sample for the overgrown region (c) and the coherently grown region (d). Micro-PL measurements for these regions (e) and (f) taken at the indicated spots.

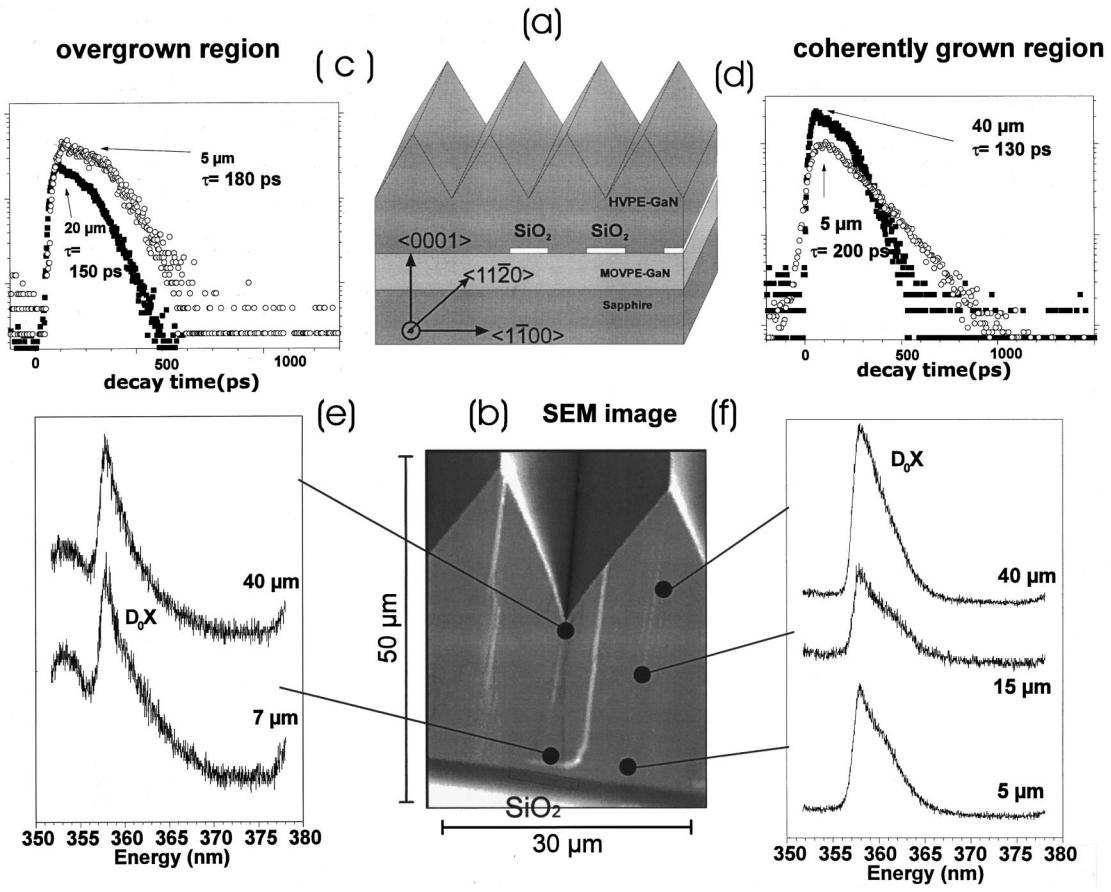

FIG. 2. Schematic structure of ELOG sample B with the SiO_2 pattern along the $\langle 11\underline{2}0\rangle$ direction (a) together with a SEM image (b) and transients taken at 358 ± 5 nm for different distances from the masks of the sample for the overgrown region (c) and the coherently grown region (d). Micro-PL measurements for these regions (e) and (f) taken at the indicated spots.

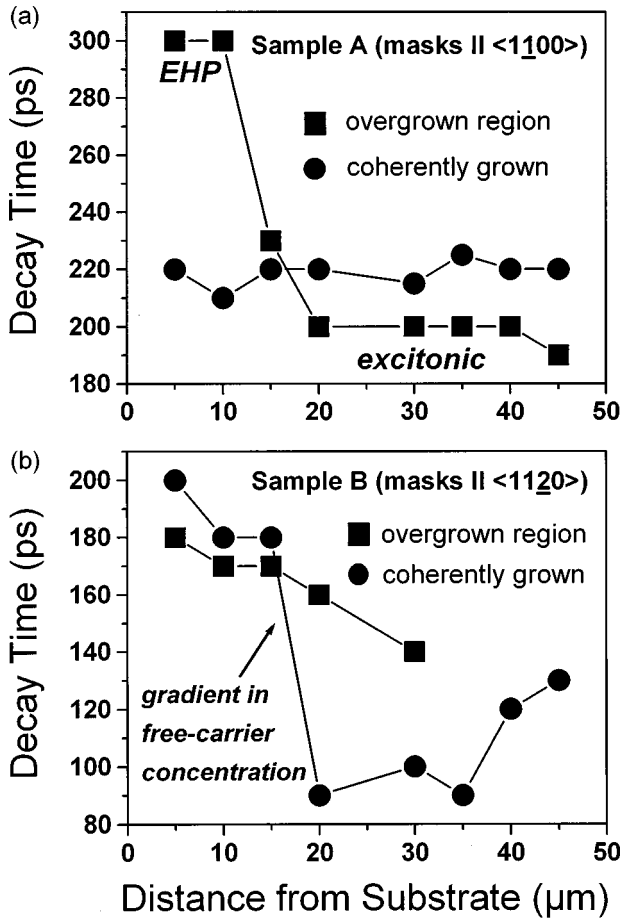

FIG. 3. Decay constants of the near-band-gap emissions as function of the distance from the substrate taken along a line between the samples surface and the substrate interface for sample A and sample B. Data points were taken in the overgrown (squares) and in the coherently grown regions (circles). The lines are guide to the eyes.

pulse with three independent exponential decays of different amplitudes. The time constants vary strongly with the local position on the samples. The transients, collected right above the SiO_2 masks and close to the surface—as shown in Figs. 1(c), 1(d), 2(c), and 2(d)—illustrate this behavior in both samples. The results of the scans in the different regions and the resulting time constants of the recombinations are summarized in Figs. 3(a) and 3(b).

In the overgrown region of sample A the time constants are almost constant with increasing distance from the substrate and sharply increased from 200 ± 10 to 300 ± 15 ps at 10 μm above the masks. This can be understood by the observed transition from excitonic to non-*k*-conserving band-to-band recombinations due to the high carrier concentration in this area. As known from highly doped wide-gap semiconductors likes CdS:In, a sharp increase to longer decay constants is observed above the Mott density.[7] For the coherently grown region constant decay times of about 220 ± 12 ps along the cross section are observed, indicating the homogeneous distribution of luminescence centers and the excellent material quality as it is consistent with the micro-PL measurements. The recombination dynamics of sample B is summarized in Fig. 3(b), exhibiting monoexponential decay with decay times from 90 ± 5 to 200 ± 10 ps. In the overgrown region, the time constants increase slightly from 150 ± 8 to 180 ± 9 ps as one approaches the substrate. The luminescence decays double exponentially, influenced by the dynamics of band-to-band transitions and excitonic processes. The slower band-to-band processes dominate the dynamics above the masks, as can be seen in micro-PL, and the faster excitonic processes dominate the decay with increasing distance from the substrate. In the coherently grown region, the decay times decrease with decreasing distance from the substrate. At 15 μm from the substrate a sharp increase to time constants of 180 ± 9 ps is observed. The effect of decreasing time constants can be explained by an increased number of incorporated impurities along the scan towards the substrate.[4] As explained by Rashba and Gurgenishvili,[8] the average distance of impurity centers compared to the exciton-impurity complex is reduced, since the number of impurities is increased. Thus, the higher the impurity concentration, the greater the Coulomb screening on the donor–exciton binding energy. The effective binding energy is lowered and so is the radiative decay time, but the bound-exciton complex still exists. This drastically changes at 15 μm from the substrate. The sharp increase in time constant is linked to a drop off in free-carrier concentration by one order of magnitude at this point.[4] It should be noted that the sharp increase in lifetime in the overgrown region of sample A is of different physical origin than in the coherently grown region of sample B. While in sample A a *different emission process* causes the increase of decay time, the reduction of impurity centers is the reason for the longer lifetimes in sample B.

Summarizing the micro-PL and time-resolved measurements, we comprehensively microcharacterized two ELO GaN samples with different orientation of the SiO_2 masks. From our findings we identified different growth regimes and different physical processes which determine the decaying times.

This work was supported by Deutsche Forschungsgemeinschaft. A.K. acknowledges an Ernst von Siemens scholarship.

[1] For a review, see S. Nakamura and G. Fasol, *The Blue Laser Diode* (Springer, Heidelberg, 1997).
[2] S. Nakamura, M. Senoh, S. Nagahama, N. Iwasa, T. Yamada, T. Matsushita, H. Kiyoku, Y. Sugimoto, T. Kozaki, H. Umemoto, M. Sano, and K. Chocho, Jpn. J. Appl. Phys., Part 2 **36**, L1568 (1997).
[3] A. Usui, H. Sunakawa, A. Sakai, and A. Yamaguchi, Jpn. J. Appl. Phys., Part 2 **36**, L899 (1997).
[4] F. Bertram, T. Riemann, J. Christen, A. Kaschner, A. Hoffmann, C. Thomsen, K. Hiramatsu, T. Shibata, and N. Sawaki, Appl. Phys. Lett. **74**, 359 (1999).
[5] A. Kaschner, A. Hoffmann, C. Thomsen, F. Bertram, T. Riemann, J. Christen, and K. Hiramatsu, Appl. Phys. Lett. **74**, 3320 (1999).
[6] P. Fischer, J. Christen, M. Zacharias, H. Nakashima, and K. Hiramatsu, Solid State Phenom. **6**, 151 (1998).
[7] C. Fricke, R. Heitz, A. Hoffmann, and I. Broser, Phys. Rev. B **49**, 5313 (1993).
[8] E. I. Rashba and G. E. Gurgenishvili, Fiz. Tverd. Tela **4**, 1095 (1962).